



## *Kepler Data Release Notes 2*

KSCI-19042

Data Analysis Working Group (DAWG)

*Jeffrey Van Cleve, Editor*

### Data Release 2

Quarter	Data Type	First Cadence MJD midTime	Last Cadence MJD midTime	Number of Cadences
0	SC	54953.028	54962.754	14280
0	LC	54953.038	54962.744	476
0	FFI	54945.732	54947.156	8
1	SC	54964.001	54997.491	49170
1	LC	54964.011	54997.481	1639

*Including Dropped Targets for the Public*

Prepared by: \_\_\_\_\_ Date \_\_\_\_\_  
Jeffrey Van Cleve, Kepler Science Office, for the DAWG (next page)

Approved by: \_\_\_\_\_ Date \_\_\_\_\_  
Jon Jenkins, Signal Processing Co-Investigator & DAWG Lead

Approved by: \_\_\_\_\_ Date \_\_\_\_\_  
Michael R. Haas, Science Office Director

These Notes are the collective effort of the Data Analysis Working Group (DAWG), composed of SO and SOC members as listed below:

Jon Jenkins, Chair

Doug Caldwell, Co-Chair

Allen, Christopher L.

Batalha, Natalie

Bryson, Stephen T.

Chandrasekaran, Hema

Clarke, Bruce D.

Cote, Miles T.

Dotson, Jessie L.

Gilliland, Ron (STSci)

Girouard, Forrest

Haas, Michael R.

Hall, Jennifer

Ibrahim, Khadeejah

Klaus, Todd

Kolodziejczak, Jeff (MSFC)

Li, Jie

McCauliff, Sean D.

Middour, Christopher K.

Pletcher, David L.

Quintana, Elisa V.

Tenenbaum, Peter G.

Twicken, Joe

Uddin, Akm Kamal

Van Cleve, Jeffrey

Wohler, Bill

Wu, Hayley Y.

Affiliations are Kepler Science Office or Science Operations Center unless otherwise noted.

## Document Control

### Ownership

This document is part of the Kepler Project Documentation that is controlled by the Kepler Project Office, NASA/Ames Research Center, Moffett Field, California.

### Control Level

This document will be controlled under KPO @ Ames Configuration Management system. Changes to this document **shall** be controlled.

### Physical Location

The physical location of this document will be in the KPO @ Ames Data Center.

### Distribution Requests

To be placed on the distribution list for additional revisions of this document, please address your request to the Kepler Science Office:

Michael R. Haas  
Kepler Science Office Director  
MS 244-30  
NASA Ames Research Center  
Moffett Field, CA 94035-1000  
Michael.R.Haas@nasa.gov

## Table of Contents

1. Introduction.....	6
2. Release Description .....	7
2.1 Summary of Contents .....	7
2.2 Pipeline Changes Since Previous Release.....	8
3. Current Evaluation of Performance .....	9
3.1 Overall.....	9
3.2 Changes in Performance Since Previous Release .....	9
3.3 Ongoing Calibration Issues .....	9
4. Data Delivered – Processing History.....	11
4.1 Overview .....	11
4.2 Pixel-Level Calibration (CAL).....	11
4.3 Photometric Analysis (PA) .....	12
4.4 Pre-Search Data Conditioning (PDC) .....	12
5. Lost Data and Systematic Errors.....	15
5.1 Momentum Desaturation.....	15
5.2 Reaction Wheel Zero Crossings .....	16
5.3 Argabrightening.....	17
5.4 Variable FGS Guide Stars .....	20
5.5 Pixel Sensitivity Dropouts .....	21
5.6 Pointing Drift .....	23
5.7 Focus Drift and Jitter.....	23
5.8 Requantization Gaps .....	24
5.9 Spurious Frequencies in SC Data with Spacing of 1/LC.....	25
5.10 Known Erroneous FITS header keywords .....	26
6. Data Delivered – Format .....	27
6.1 FFI.....	27
6.2 Light Curves .....	27
6.3 Pixels .....	28
6.4 Time and Time Stamps.....	28
7. References .....	28
8. List of Acronyms and Abbreviations .....	34
9. Contents of Supplement.....	37

## 1. Introduction

These notes have been prepared to give Kepler users of the Multimission Archive at STScI (MAST) a summary of how the data was collected and prepared, and how well the data processing pipeline used to produce the data is functioning on flight data. They will be updated for each release of data to either the MAST ftp site, or the public archive. They are not meant to supplant the following documents:

1. **Kepler Instrument Handbook** (KIH, KSCI-19033) provides information about the design, performance, and operational constraints of the Kepler hardware, and an overview of the pixel data sets available. It was released on July 15, 2009, and will publicly available on MAST on 10/15/2009. The user should refer to the KIH for a glossary and acronym list.
2. **Kepler Data Analysis Handbook** (KDAH) describes how these pixel data sets are transformed into photometric time series by the Kepler Science Pipeline, the theoretical basis of the algorithms used to reduce data, and a description of residual instrument artifacts after Pipeline processing. The initial release of the KDAH is expected on 11/15/09.
3. **SOC Tools User's Guide** describes the data and model retrieval tools written by the SOC, which offer unambiguous access to current calibration data and models, and to science data at various stages of processing which are not available through MAST. This User's Guide will only be available to and useful for Science Team members who visit the SOC at the invitation of the Science PI as the tools only exist in the SO/SOC.
4. **Kepler Archive Manual** (KDMC-10008) describes file formats and the availability of data through MAST. The Archive Manual is also expected to be available on MAST [http://archive.stsci.edu/kepler/manuals/K\\_archive\\_manual\\_v4\\_083009.htm](http://archive.stsci.edu/kepler/manuals/K_archive_manual_v4_083009.htm)

The format of these Release Notes has become more structured than that of the first Notes (of 7/17/09), in the belief that they will be more maintainable. However, much of the content from these earlier notes is reproduced here for the user's convenience. Users unfamiliar with the data processing pipeline should read Section 4 first. A list of acronyms and abbreviations is in Section 8.

Data which would be unwieldy to print in this document format are included in a zip file, the Data Release Notes #2 Supplement, which will be released with this document. Supplement files are called out in the text, and a README file in the zip file also gives a brief description of the files contained. Supplement files are either ASCII or FITS format.

Note on dates and cadence numbers in these Notes: figures, tables, and supplement files will use MJD as the preferred time base. Cadences are absolutely enumerated with cadence interval numbers (CIN), which increment even when no cadences are being collected, such as during downlinks and safe modes. Cadence interval numbers are used in SOC intermediate data products and appear as the keywords LC\_INTER and SC\_INTER in the headers of FITS cadence files (not available through MAST). Users may also find useful the *relative cadence index* (RCI), which is the cadence number counted from the beginning of a quarter. For example, the first LC of Q1 would have an RCI = 1 and CIN = LC\_INTER = 1105 while the last LC of Q1 has RCI = 1639 and CIN = LC\_INTER = 2743.

## 2. Release Description

A *data description* refers to the data type and observation interval during which the data was collected. The observation interval is usually *quarters*, indicated by Q[n], though Q0 and Q1 are 10 days and one month, respectively, instead of 3 months as will be the case for the rest of the mission. The *data processing* descriptor refers to exactly how the data was processed in the Pipeline, including the software version and associated set of input parameters. The same data will, in general, be reprocessed as the software improves, and will hence be the subject of multiple releases. The combination of data and data processing descriptions defines a *data product*, and a set of data products simultaneously delivered to MAST for either public or proprietary (Science Team or GO) access is called a *data release*. The first release of data products for a given set of data is referred to as “new,” while subsequent releases are referred to as “reprocessed.”

For the time being, the data processing descriptor is the internal Kepler Science Operations Procedure (KSOP) number used to request the data processing and the subsequent release. The KSOP refers to software change requests (KSOCs) describing how the processing is different from that of previous releases. At present, this information is not captured in the FITS headers, and it is up to users to associate the FITS files of a given release with the corresponding Release Notes which summarize the KSOPs and KSOCs.

In the near future, it is expected that a few keywords will be added to the light curve FITS headers so users can know unambiguously that they have the best (presumably most recent) release, and identify the data products used in their papers and communications with the Science Office. A FITS file would then be matched up with the corresponding Release Notes, which would tell the user more about the data and its processing.

Data Release 2 is “browse quality” data. It is meant to give users the opportunity to examine the data for possibly interesting science, as well the opportunity to improve flight system operations and SOC data analysis for future releases by noticing and documenting artifacts in the raw data or the data analysis. It is not meant to be publication quality data as-is.

### 2.1 Summary of Contents

**Table 1: Contents of Release 2. CIN is the cadence interval number described in Section 1. ‘For’ indicates who will have access to the data in this release, with the exception of the Dropped Targets for Q0 and Q1, which will be available to the public. The Table on the cover page is a subset of this Table.**

Quarter	For	Data Type	new?	Code KSOP	Pipe-line KSOP	Export KSOP	First Cadence MJD midTime	Last Cadence MJD midTime	CIN Start	CIN End	Num Cads
0	ST	SC	new	215	229	253	54953.028	54962.754	5500	19779	14280
0	ST	LC	reproc	215	229	225, 247	54953.038	54962.744	568	1043	476
0	public	FFI	new	221	221	226, 247	54945.732	54947.156	N/A	N/A	8
1	ST	SC	new	215	227	254	54964.001	54997.491	21610	70779	49170
1	ST	LC	new	215	227	254	54964.011	54997.481	1105	2743	1639

Notes:

Calibrated “golden” FFIs were processed under KSOP-226. They are called “golden” FFIs since they were collected under conditions of excellent thermal and pointing stability during Commissioning, using the same integration parameters as the Long Cadence science data, and after the final focus settings were achieved. Aside from the exception of cosmic ray cleaning, which is not available for FFIs, the same CAL processing (Section 4) has been applied to these images as to the light curves in this release. Thus, these images are good representations of what targets and their neighborhoods look like. Eight are available, so users can average them to look at faint sources, difference them in various ways to better understand noise and systematics, or search for variable stars which are currently not LC targets.

The Long Cadence data collected during the CDPP Commissioning Activity (C-043) have been reprocessed under KSOP-229. The data description (formerly “CDPP”) will subsequently be “Quarter Zero” (Q0) since it has become increasingly confusing to have a data set and a key performance metric share the same name.

Release 3, comprising Q2 (MJD 55002 – 55090) and reprocessed Q1 and Q0 data, is expected in mid-January 2010.

## **2.2 Pipeline Changes Since Previous Release**

The Computer Software Configuration Items (CSCIs) comprising the science data analysis Pipeline are described briefly in Section 4. Users unfamiliar with the Pipeline should read Section 4 before reading this Section and Section 3.

The CAL data analysis has not been repeated in the reprocessed Q0 LC data, as no changes were made to CAL since the previous release. The changes in PA and PDC, labeled by their internal change request numbers (KSOC-*nnn*) were:

1. KSOC-388: Detect Argabrightening events (Section 5.3) and gap data in PA
2. KSOC-387: Smoothing Option for Motion Time Series [PA/PDC/DV]
3. KSOC-355: Exclude variable stars from PA motion polynomial fit, brightness and encircled energy metrics
4. KSOC-297: Exclude out of family centroids from PA motion polynomial fit
5. KSOC-349: PRF smoothing bug
6. KSOC-401: PA Cosmic Ray cleaning. Prior method: SVD decomposition and deprojection of motion components before thresholding. Revised method: use median filtering and MAD (median absolute deviation) thresholding for background and target cosmic ray removal.

The PA and PDC versions and input parameters can be unambiguously referenced by their Pipeline Instance Identifier (PID), which for example is 359 for both PA and PDC in the Q1 LC data.

### 3. Current Evaluation of Performance

#### 3.1 Overall

The CDPP performance has been discussed by Borucki et al. [1]. In a nutshell, they conclude that the joint performance of the instrument and the data analysis Pipeline gives noise on 0.5 hr timescales between one and two times the expected value, for stars which are indeed dwarfs and not giants or otherwise peculiar. Nonetheless, the following cautions apply for interpreting data at this point in our knowledge of the Instrument's performance:

1. Many stars remain unclassified until Kepler and other data can be used to ascertain whether they are giants or otherwise peculiar. Since giant stars are intrinsically variable at the level of Kepler's precision, they must be excluded from calculations of CDPP performance.
2. Given the instrument artifacts discussed in detail in the KIH, it is not generally possible to extrapolate noise as  $1/\sqrt{\text{time}}$  from the 0.5 hr results on those channels afflicted by artifacts which are presently not corrected or flagged by the Pipeline.
3. Stellar variability and other instrumental effects may not be white noise processes.

Example published data is shown in [2].

The Photometer Performance Assessment (PPA) tool formally calculates CDPP on 6 hr timescales. The median value for Q1, calculated for all targets with magnitude between 11.5 and 12.5, is 79 ppm, while the 10<sup>th</sup> percentile is 30.1 ppm. It is believed that the 10<sup>th</sup> percentile value is a better representation of instrument and Pipeline performance than the median value, once astrophysical factors are controlled for. Thus, the CDPP metric on 6hr timescales is ~50% noisier than the requirement of 20 ppm for 12<sup>th</sup> magnitude stars, in agreement with the 0.5 hr running difference results.

#### 3.2 Changes in Performance Since Previous Release

Significant improvements to PDC's outputs have been realized as a consequence of flagging Argabrightening events (Section 5.3) and smoothing the motion. PDC is no longer introducing transit time scale systematics into the corrected flux data through the cotrending process, but it is not yet correcting systematics on those time scales. The corrected (output of PDC) results have lower high-frequency ( $>0.15 \text{ hr}^{-1}$ ) noise than the Release 1 corrected light curves, and are not overly sensitive to pointing errors. Systematic errors at lower frequencies ( $<0.15 \text{ hr}^{-1}$ ) remain apparent, and still present difficulties for the automated detection of transits.

#### 3.3 Ongoing Calibration Issues

Topics under consideration by the DAWG which may in the near-term change calibration parameters or methods include:

1. Identify additional flight system state variables which can be used to detrend the data in PDC. Currently, only row and column motion time series are being detrended. Other example variables could include electronics and optics temperatures. The same algorithm (SVD) would be used, but with an expanded set of basis functions.
2. Identify trends and periodicities in fluxes and centroids in both science and Fine Guidance Sensor data (Sections 5.4 and 5.5)
3. Implement improved methods for identifying and removing phase modulated harmonics from a time series (of either astrophysical or instrumental origin)

4. Characterize the in-orbit change of focus (Section 5.7) and develop a mitigation strategy, either by refocusing the telescope or by accounting for time-variable PSFs (as has been done for Hubble data by Gilliland).

Calibration and data analysis issues related to the focal plane and its electronics are discussed in the "Artifacts" section of the Instrument Handbook.

## 4. Data Delivered – Processing History

### 4.1 Overview

The delivered FITS files were processed as shown in simplified form in Figure 1. What is referred to as “raw” flux time series is the result of calibrating pixels, estimating and removing sky background, and extracting a time series from a photometric aperture. The “corrected” flux time series has been decorrelated against known system state variables, such as pointing.

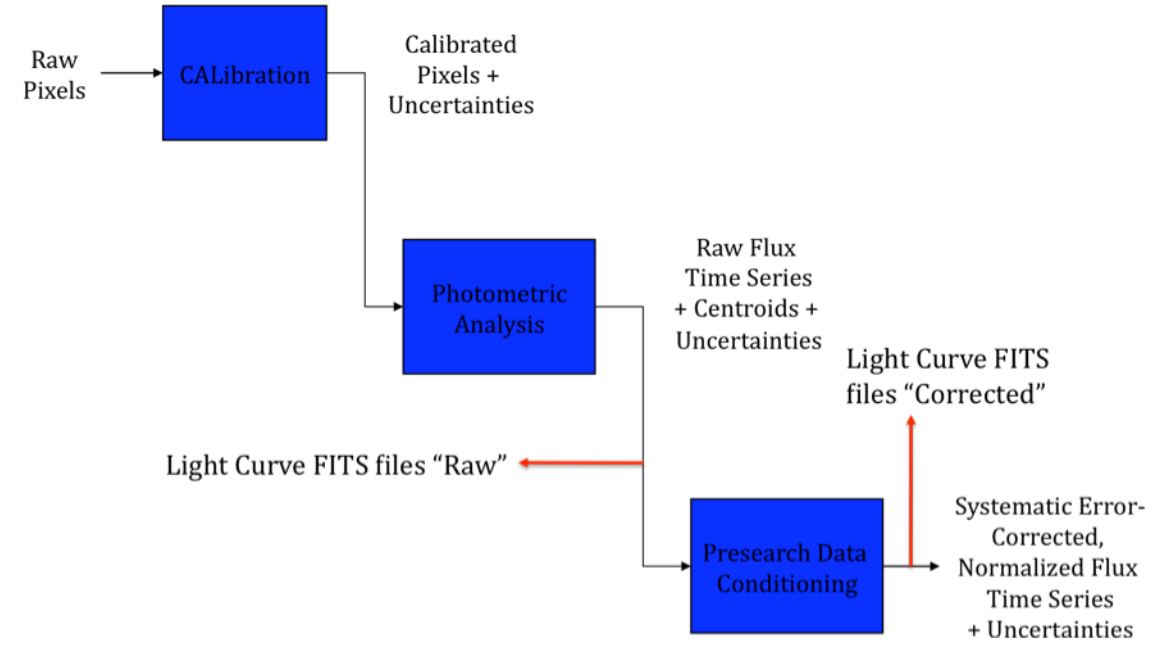


**Figure 1: Processing of Data from Raw Pixels To Flux Time Series. Red arrows indicate the origin of the data in the delivered light curve FITS files.**

### 4.2 Pixel-Level Calibration (CAL)

The first step, pixel calibration (software module CAL), performs the pixel level calibrations shown in Figure 2.

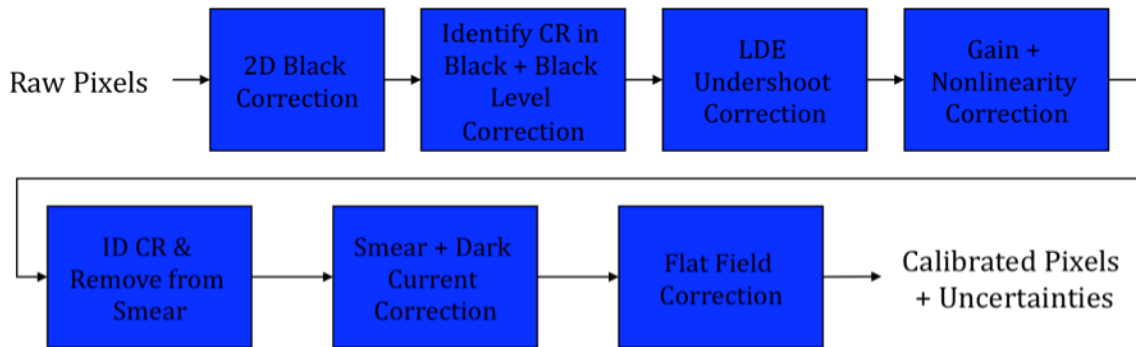


**Figure 2: Pixel Level Calibrations Performed in CAL. See the Instrument Handbook for a discussion of signal features and image contents processed in CAL.**

### 4.3 Photometric Analysis (PA)

After the pixels are calibrated, Photometric Analysis (PA)

1. Cleans cosmic rays
2. Removes background
3. Extracts flux from each aperture. In release 2, the flux is the sum of pixels in the optimal aperture (Simple Aperture Photometry, SAP), rather than an optimal extraction (OAP).
4. Calculates first-moment centroids for each target from the pixels in the optimal aperture.
5. Sets gap indicators as for cadences with either a momentum dump (Section 5.1) or an Argabrightening (Section 5.3). The gapped cadences have all  $-\text{Inf}$  values in the FITS light curve files, except for the first two columns: time and cadence number.

#### *Notes*

Photometer Performance Assessment stellar targets (label: PPA\_STELLAR) uses Pixel Response Function (PRF) fitting to calculate centroids. If the PRF-based centroiding failed for a given PPA\_STELLAR target and cadence, then there is no centroid for that target and cadence. Roughly 17,000 targets, or 10% of the total, are classified as PPA\_STELLAR. The PPA\_STELLAR targets used in Q1 are listed in the Supplement. For all other targets, first-moment (also known as flux-weighted) centroids are used. The first-moments centroids are considered informational, and are meant to be used to look for correlations between centroid motion and flux time series. Users wishing to do precise centroiding for non-PPA\_STELLAR targets need to consider the distribution of flux from non-target sources in the optimal aperture pixels or use the PRFs provided in the KIH Supplement and duplicated in the Supplement to these Notes.

There is no identification of bad pixels in PA in Release 2, nor is there any exclusion, gapping or other treatment of known bad pixels. Bad pixels may be identified in future releases. The treatment of bad pixels is TBD, and may depend on how the pixel is bad (high read noise, unstable photoresponse, low photoresponse, etc.) and its location in the target aperture.

The output of PA is called 'raw' in the light curve FITS file, even though it is the sum of 'calibrated' pixels.

### 4.4 Pre-Search Data Conditioning (PDC)

Pre-Search Data Conditioning, applies these steps:

1. Resample ancillary data to match the sampling rate of LC and SC data.

2. Co-trend target flux time series against ancillary data using Singular Value Decomposition (SVD) to remove common linear/non-linear deterministic trends
3. Remove the excess flux in the optimal aperture for each target due to (estimated) crowding.
4. Identify and remove impulsive outliers
5. Fill gaps in conditioned flux time series. Gap filling is for further analysis for internal SOC purposes only; MAST users are given –Infs in the FITS light curve files for the gap Cadences rather than the filled values.

Notes

In Release 2, PDC uses only row and column centroid motion time series as ancillary data for co-trending against flux time series. Other ancillary data, such as LDE board and reaction wheel housing temperature (Section 5.7) will be included in the analysis set as our understanding of the flight system improves.

The crowding metric is the fraction of non-zodiacal light in an aperture which comes from the target star. For example, a crowding metric of 1 means that all the light in an aperture comes from the target, so the light curve needs no correction. A crowding metric of 0.5 means that half the light is from the target and half from other sources, so half the flux must be removed before the correct relative transit depth is obtained. The crowding metrics used for PDC Step 4 in the release 2 pipeline processing were not correct, and that the corrected flux levels for crowded targets are therefore also not correct. In general, too much excess flux has been removed from crowded targets so that apparent transit depths in the corrected flux are too large. The error increases as the crowding increases. This error will be corrected for Release 3. Note that the 'raw' flux time series are *not* corrected for crowding.

PDC detects outliers in the target flux time series after first identifying and isolating astrophysical events. A median filter is applied to the time series after the removal of obvious astrophysics, and the residual is determined by subtracting the median series from the target flux series. A robust running mean and standard deviation of the residual is calculated and points more than  $6\sigma$  from the mean are excluded.

Figure 3 shows the efficacy of steps 1-3 on output from the End-to-End Model (ETEM).

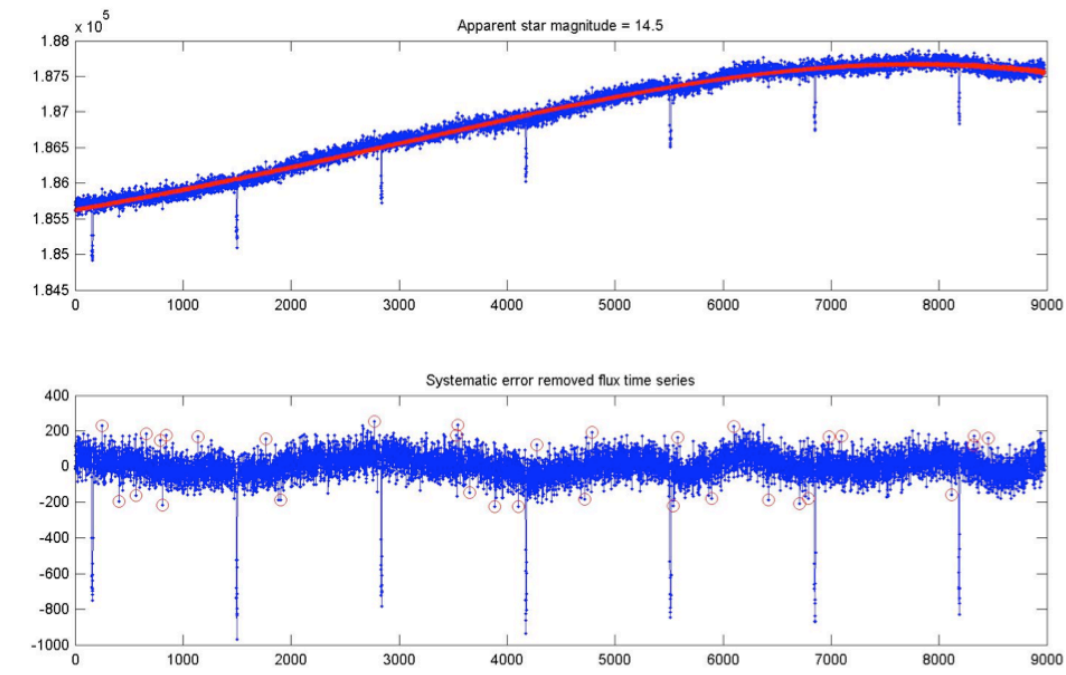


**Figure 3: PDC trend removal example using synthetic data. Upper panel: Data in blue and trend line to be removed from data in red. Giant-planet transits were masked out before trend fitting. Lower panel: Residual after removal of trend. Outliers are marked by red circles.**

The output of PDC is referred to as ‘corrected’ data in the delivered files. Users are cautioned that systematic errors remain, and their removal is the subject of ongoing effort as described in Section 3.3. Users may look at the ‘corrected’ data for indications of possibly interesting phenomena, but are strongly advised to use pixel data or uncorrected flux time series as inputs for their own analysis, for near-term publication purposes.

## 5. Lost Data and Systematic Errors

In this Section, we discuss cadences which are essentially lost to high-precision photometry due to planned or unplanned spacecraft events. While most of these events are either reported by the spacecraft or detected in the Pipeline and gap-filled, this Section reports events at lower thresholds than the Pipeline which may be of interest to some users.

We also discuss systematic errors arising in on-orbit operations, most of which in principal will be removed from flux time series by PDC (Section 4). However, since the Release 2 data is detrended only against centroid motion, other telemetry items which may be used for detrending the data in future releases are included so that users can at least qualitatively assess whether features in the time series look suspiciously like features in the telemetry items. In addition, PDC corrects systematic effects only in the flux time series, and this Section may be useful for users interested in centroids or pixel data.

Particularly annoying and unexpected phenomena are written up as Kepler Anomaly Reports (KARs) or SOC change requests (KSOCs). While KARs and KSOCs are not available to users, the KAR number is listed at the end of each Section for Science Office internal reference.

### 5.1 Momentum Desaturation

Solar radiation torque causes angular momentum to build up in the reaction wheels, which then must be desaturated by thruster firings when the wheels spin up to their maximum operating RPM. Desats are scheduled to occur every 3.0 days. The spacecraft (S/C) is not designed to maintain Fine Point control during these events, and enters Coarse Point mode. The subsequent image motion is sufficient to spoil the photometric precision of data collected during desats, and a few minutes after desats during which the S/C restores Fine Point control. One LC and several SCs are affected for each desaturation.

In Release 2, only data collected during the momentum dump itself were gapped, while data which was collected in Coarse Point during the recovery to Fine Point control after completion of the momentum dump were not gapped. Long Cadences are long enough so that the momentum desat Cadence also contains the entire recovery to Fine Point, so no additional gapping is required. The gapped cadences have the value  $-\text{Inf}$  in the delivered light curve files, but appear in the uncalibrated and calibrated pixels. They are listed in Table 2 so that users of time series will know which cadences have been gap-filled, and users of pixel data will know which cadences to exclude from their own analyses.

In Short Cadence, on the other hand, there are several Cadences which were collected in Coarse Point, but not gapped by the Pipeline in Release 2. These more numerous Coarse Point SC cadences are listed in the Supplement so users can exclude them from their analyses of both light curves and pixels.

**Table 2: Long Cadences which were not in Fine Point. CIN = Cadence Interval Number, RCI = Relative Cadence Index, isMmntDmp = Cadence flagged as occurring during a momentum dump and gapped by the Pipeline in Release 2. All LCs not in FinePoint are flagged, since they are identical to momentum dump cadences. This is not true for Short Cadences.**

Q0	LC	CIN	RCI	Date (MJD)	isMmntDmp
		703	136	54955.79669	1
		848	281	54958.75956	1
		950	383	54960.84379	1

Q1 LC

CIN	RCI	Date(MJD)	isMmntDmp
1246	142	54966.89213	1
1392	288	54969.87544	1
1538	434	54972.85874	1
1684	580	54975.84205	1
1830	726	54978.82535	1
1976	872	54981.80866	1
2122	1018	54984.79196	1
2268	1164	54987.77527	1
2414	1310	54990.75857	1
2560	1456	54993.74188	1
2706	1602	54996.72518	1

## 5.2 Reaction Wheel Zero Crossings

Another aspect of S/C momentum management is that at least one of the reaction wheels crosses zero angular velocity from time to time. This causes the affected wheel to rumble and degrade the pointing on timescales of a few minutes. The primary consequence is an increased noise in the short cadence centroid time series, with a resulting increase in noise in the pixel and flux time series. During zero crossings, we observe negative spikes of order  $10^{-3}$  in all SC relative flux time series; in many cases this results in poor aperture photometry for the cadences in question, and these cadences must be excluded from further analysis. The severity of the impact to the SC flux time series seems to vary from target to target, with all SC targets showing some impact to the centroid and pixel time series. The impact on long cadence data is much less severe in both amplitude and prevalence.

The problems with the flux time series are believed to be significantly exacerbated by our cosmic ray removal inappropriately removing flux during the zero crossings, and hence can be remedied in a future version of the Pipeline. Zero crossing events in Q1, defined as the time from first to last zero in the event, are shown in Table 3. There were no zero crossings in Q0.

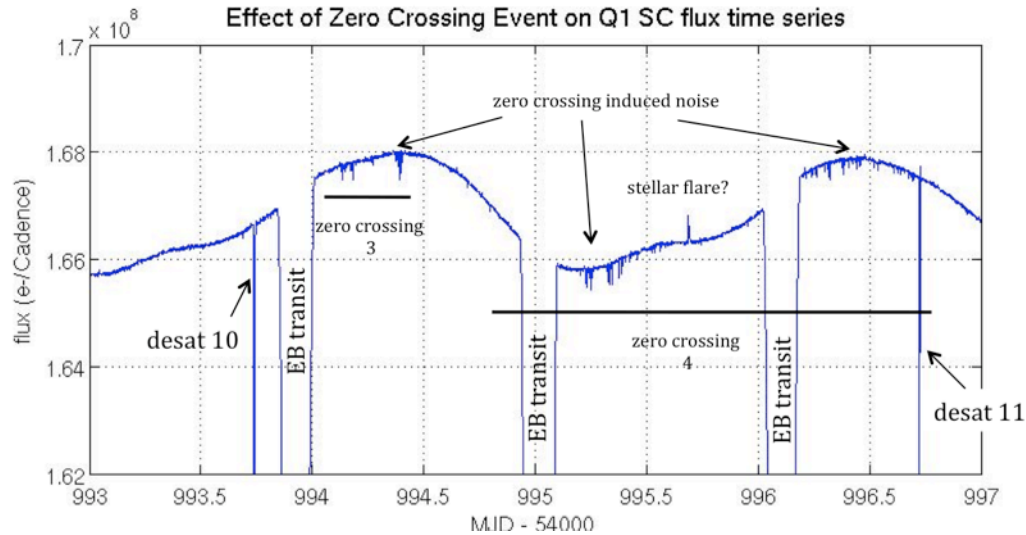


**Figure 4: An SC Example with (possibly) Interesting Astrophysics. Cadences identified as gaps by the Pipeline are omitted from this plot, but some out of Fine Point Cadences remain after momentum dumps (Section 5.1), as labeled above. If the stellar flare had fallen on one of the noisy regions, it might have been missed. The target is an eclipsing binary, with the transits indicated by ‘EB transit’.**

**Table 3: Zero crossing events in Q1, defined as the time from first to last zero in the event. Corresponding Q1 relative cadence indices are shown. There were no zero crossings in Q0.**

Q1	zero-crossing	events	LC RCI	LC RCI	SC RCI	SC RCI	
Event #	MJD start	MJD end	start	end	start	end	Event description
1	54985.200	54985.344	1037	1046	31124	31336	reaction wheel 1, follows desat 7
2	54985.390	54985.625	1047	1059	31403	31749	reaction wheel 2, follows desat 7
3	54994.056	54994.458	1471	1492	44126	44717	reaction wheel 1, follows desat 10
4	54994.875	54996.750	1511	1604	45329	48082	reaction wheel 2, follows desat 10

Reference: KAR-529

### 5.3 Argabrightening

*Argabrightening*, named after its discoverer V. Argabright of BATC, is a presently unexplained diffuse illumination of the focal plane, lasting on the order of a few minutes. It is known to be light rather than an electronic offset since it appears in calibrated pixel data from which the electronic black level has been removed using the collateral data. It is not a result of gain change, or of targets moving in their apertures, since the phenomenon appears with the same amplitude in background pixels (in LC) or pixels outside the optimal aperture (in SC) as well as stellar target pixels. Many channels are affected simultaneously, and the amplitude of the event on each channel is many standard deviations above the trend. The method of detection is to fit a trend line to calibrated background (LC) or out-of-optimal-aperture (SC) pixels, fit a parabola, smooth the residual, and look for outliers in the difference between the residual and the smoothed residual. The Pipeline identifies Argabrightenings with this method, and subsequently treats

those cadences as gaps. The Pipeline does not identify multichannel events, but instead processes each channel in isolation.

The Pipeline uses a rather high threshold of 100x the median absolute deviation (MAD) for LC and 60x for SC. While it appears that background subtraction has mostly removed this phenomenon from the delivered Long Cadence data, the residual effect has not been proven to be negligible in all cases, especially in Short Cadence data. There may also be significant Argbrightening events in both LC and SC, which do not exceed the default thresholds.

This Section gives a summary of events which exceed the 10x MAD threshold on at least 11 channels, so that the user may consider whether some cadences of interest might be afflicted by Argbrightening, but not identified as such by the Pipeline and gapped (i.e., -Inf in the light curve file). The Supplement contains channel-by-channel results.

**Table 4: Q0 LC Argbrightening Events with amplitude greater than 10x the median absolute deviation (MAD), which occurred simultaneously on at least 11 of the 84 channels. The columns are 1) CIN = Cadence Interval Number for Argbrightening Cadences, 2) RCI = Relative Cadence Index for Argbrightening Cadences, 3) Date = Arg Cadence mid-Times, MJD, 4) Mean SNR over Channels of Arg Event, 5) N\_chan = Channels exceeding threshold in Arg Cadence, 6) N\_pipe = Channels exceeding default (Pipeline) threshold in ArgCadence. MAD is calculated on a channel-by-channel basis. Number of Arg Events Detected: 11 Events Per Month: 34.0**

CIN	RCI	Date (MJD)	MeanSNR	N_chan	N_pipe
586	19	54953.40596	28.2	64	0
619	52	54954.08027	27.4	84	0
647	80	54954.65241	8.8	27	0
790	223	54957.57441	105.0	84	52
860	293	54959.00476	7.8	20	0
901	334	54959.84254	29.9	84	0
914	347	54960.10818	48.7	70	1
915	348	54960.12861	17.5	60	0
958	391	54961.00726	22.2	67	0
972	405	54961.29333	956.5	84	84
973	406	54961.31376	19.5	63	0

**Table 5: Same analysis as Table 4, for Q0 SC. Note consecutive detections of the largest events. Number of Arg Events Detected: 19 Events Per Month: 58.6**

CIN	RCI	Date (MJD)	MeanSNR	N_chan	N_pipe
6058	559	54953.40834	17.8	47	2
6059	560	54953.40902	16.2	48	0
7034	1535	54954.07311	35.1	80	5
7870	2371	54954.64253	8.6	27	0
7911	2412	54954.67046	8.2	27	0

12179	6680	54957.57748	137.5	82	79
13029	7530	54958.15643	6.3	12	0
14282	8783	54959.00987	11.0	43	0
15509	10010	54959.84561	41.8	82	15
15898	10399	54960.11056	68.7	70	51
15932	10433	54960.13372	21.1	60	2
17205	11706	54961.00078	7.4	17	0
17206	11707	54961.00147	13.3	49	0
17207	11708	54961.00215	6.6	25	0
17647	12148	54961.30184	974.5	82	82
17648	12149	54961.30252	284.4	82	81
17649	12150	54961.30320	35.0	77	8
17650	12151	54961.30388	12.4	40	1
17651	12152	54961.30456	5.2	18	0

**Table 6: Same analysis as Table 4, for Q1 LC. Note that the total number of events in this 31-day period is about 1.5x the number of events in the 10 days of Q0, suggesting a decrease in event frequency with time.**

CIN	RCI	Date (MJD)	MeanSNR	N_chan	N_pipe
1149	45	54964.91007	11.5	59	0
1170	66	54965.33918	32.2	84	0
1230	126	54966.56519	10.1	45	0
1271	167	54967.40297	7.9	26	0
1852	748	54979.27489	13.0	60	0
1943	839	54981.13435	17.0	74	0
2082	978	54983.97462	27.8	84	0
2091	987	54984.15852	351.6	84	81
2146	1042	54985.28237	23.4	76	0
2236	1132	54987.12139	18.1	75	0
2282	1178	54988.06134	397.2	84	84
2367	1263	54989.79819	5.0	11	0
2421	1317	54990.90161	5.5	12	0
2498	1394	54992.47499	3.3	12	0
2559	1455	54993.72144	28.0	84	0
2735	1631	54997.31776	6.3	27	0

**Table 7: Same analysis as Table 4, for Q1 SC.**

CIN	RCI	Date (MJD)	MeanSNR	N_chan	N_pipe
22952	1343	54964.91518	7.0	15	0
23586	1977	54965.34701	18.1	74	0
44038	22429	54979.27727	7.3	18	0
46769	25160	54981.13741	7.1	20	0
50932	29323	54983.97292	11.3	52	0
51205	29596	54984.15886	77.0	84	58
51206	29597	54984.15954	116.2	78	61
51207	29598	54984.16022	10.0	16	4
52852	31243	54985.28067	13.8	56	0
56921	35312	54988.05214	215.9	84	83
56922	35313	54988.05282	20.5	75	1
65246	43637	54993.72247	11.8	55	0

Reference: KAR-479

#### **5.4 Variable FGS Guide Stars**

The first-moment centroiding algorithm used by the FGS did not originally subtract all of the instrumental and sky background from the FGS pixels. Thus, the calculated centroid of a star depended on its flux when the star was not located at the center of the centroiding aperture. Variable stars then induced a variation in the attitude solution calculated from the centroids of 40 guide stars, 10 in each FGS module. The Attitude Determination and Control System (ADCS), which attempts to keep the calculated attitude of the S/C constant, then moved the S/C to respond to this varying input, with the result that the boresight of the telescope moved while the ADCS reported a constant attitude. Science target star centroids and pixel time series, and to a lesser extent aperture flux, then showed systematic errors proportional to the FGS star flux variation, as shown in Figure 5. The FGS variable star light curves are included in the Supplement.

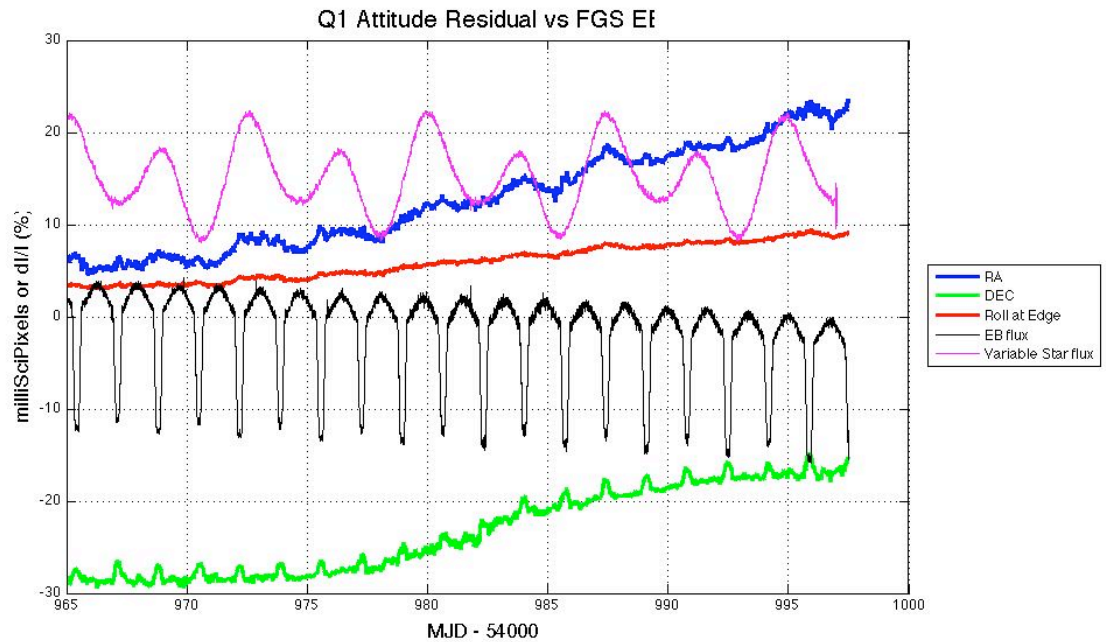


**Figure 5: Quarter 1 attitude residual and the light curves of two variable FGS guide stars vs. time. The Figure shows that guide star variability leads to pointing errors with transit-like features which can possibly be transferred to the light curves of science targets. One of the stars is an eclipsing binary (EB), while the other is an intrinsic variable. The EB flux is correlated with a pronounced transit-like signal in DEC, while the intrinsic variable star's flux is correlated with a sinusoidal component of the RA residual. The long-term trends are discussed in Section 5.6.**

The most egregious variables were replaced with quieter stars at the start of Quarter 2 (6/20/2009). While at least one intrinsic variable star and one eclipsing binary (EB) remain in the FGS, the centroiding algorithm has been updated to remove all of the instrumental background after the start of Quarter 3 (9/19/2009), greatly diminishing the effect of stellar variability on calculated centroids. The sky background will still not be removed, but is expected to be negligible.

Reference: KAR-485

## 5.5 Pixel Sensitivity Dropouts

Space-based focal planes respond to cosmic ray (CR) events in several ways:

1. A transient response is induced by the charge deposited by the CR, and is cleared by the next reset (destructive readout) of the pixel.
2. Medium-term alteration of detector properties, which recover to their pre-event values after some time and resets without annealing.
3. Long-term alteration of detector properties, which are only restored by annealing the focal plane
4. Permanent damage

Typically, type 3 and 4 effects are caused by non-ionizing energy loss (NIEL), or "knock-on" damage, which can be caused by any baryonic particle.

Type 1 effects are removed by the Pipeline's CR detection algorithm. At this point in the mission, type 3 effects do not appear to be serious enough to warrant the disruption of the observing schedule that would be caused by annealing, and both type 3 and type 4 effects will be mitigated by updating the bad pixel map used for calibration. Thus, only type 2 effects are present in the data at a significant level, and are not yet corrected by the Pipeline.

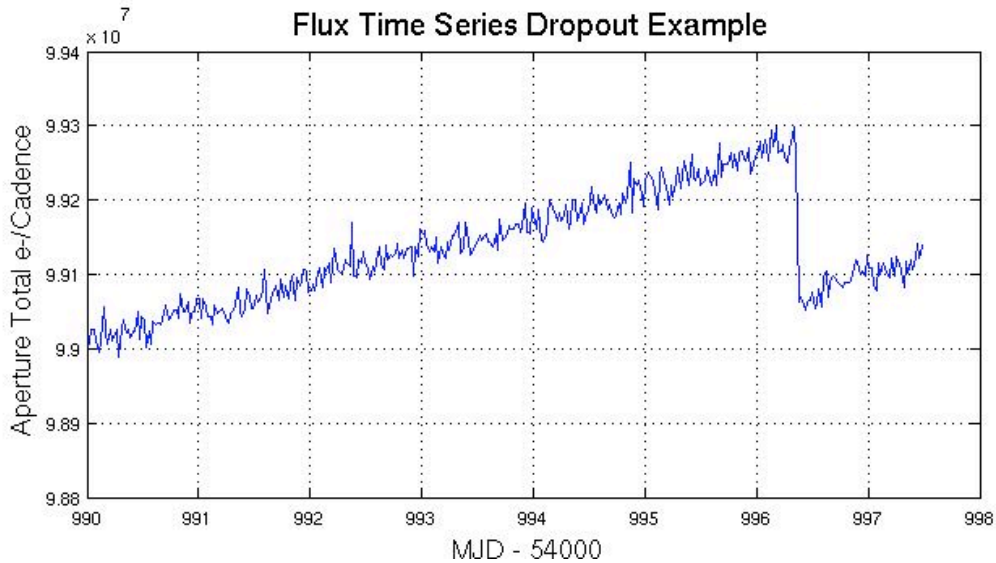


**Figure 6: Flux Time Series showing discontinuity after large CR event (next Figure). Target: KeplerID = 7960363, KeplerMag = 13.3. Processing: PA output = "raw" flux time series in MAST. CR hits have been removed by the Pipeline.**

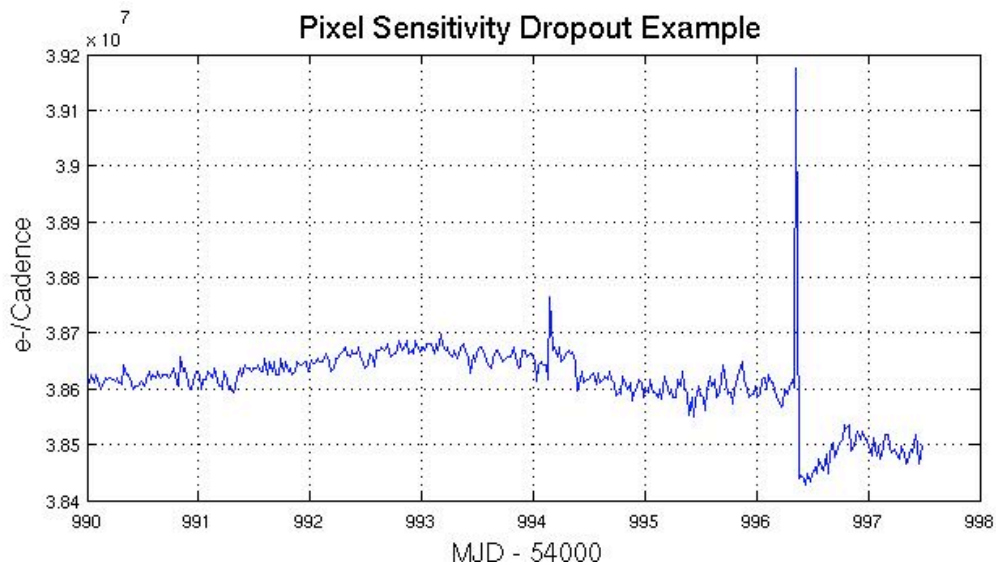


**Figure 7: Same event as for the previous Figure, but seen in an individual pixel (#15) in the aperture. CRs have not been removed by the Pipeline at this stage of processing. Data Product: CAL output = "calibrated pixels" in MAST.**

Other events can cause discontinuities in pixel and photometric time series, but such events did not occur during Q0 or Q1. They will be discussed in the KDAH and the release notes for Q2.

Reference: S. Bryson, SO/SOC and KSOC-485.

### **5.6 Pointing Drift**

Daily reference pixels are used by the SOC/SO to measure S/C attitude. The SOC PDQ software uses centroids of 3-4 stars per module/output to determine the measured boresight attitude compared with the pointing model (which accounts for differential velocity aberration). The PDQ measured attitude residuals (ra, dec, roll) for Q1 are shown in Figure 5. The plot shows an attitude drift of ~30 mpix (RSS of RA, DEC, and roll) over 31 days.

The SO is concerned that continued attitude drift could invalidate target aperture definitions and may lead to large photometric errors. Commencing in Q2, small attitude adjustments ("tweaks") are performed when the attitude error exceeds 30 mpix. While the tweaks correct the pointing, they do introduce discontinuities into the data which were not anticipated in the Pipeline. Fortunately, there are no tweaks in the Q0 and Q1 data.

Reference: KAR-485, KAR-503, and KAR-547.

### **5.7 Focus Drift and Jitter**

Examination of Q1 data reveals that many of the science targets exhibit non-sinusoidal oscillations in their flux time series with a period near 3.2 hours. The behavior is less frequent at the beginning of Q1 and becomes progressively worse with time. Initially, this phenomenon is associated with desaturation activities, but becomes nearly continuous about 15 days into the observations.

This oscillation is observed in platescale metrics local to each mod/out defined by the motion of target star centroids relative to one another over time. While this oscillation can be observed in the bulk drift of the target centroids on each Mod/Out, the FGS eclipsing binary signature that is so prevalent in the drift terms (Section 5.4) is absent in the fitted plate scale term. This indicates that we are seeing a change in focus at timescales of 3.2 hours and that the behavior appears to be initiated by the desat activities. Reaction wheel temperature sensor with the mnemonics TH1RW3T and TH1RW4T have the same time signature, but the physical mechanism by which it is coupled to plate scale is still under discussion. This temperature sensor telemetry is provided in the Supplement.

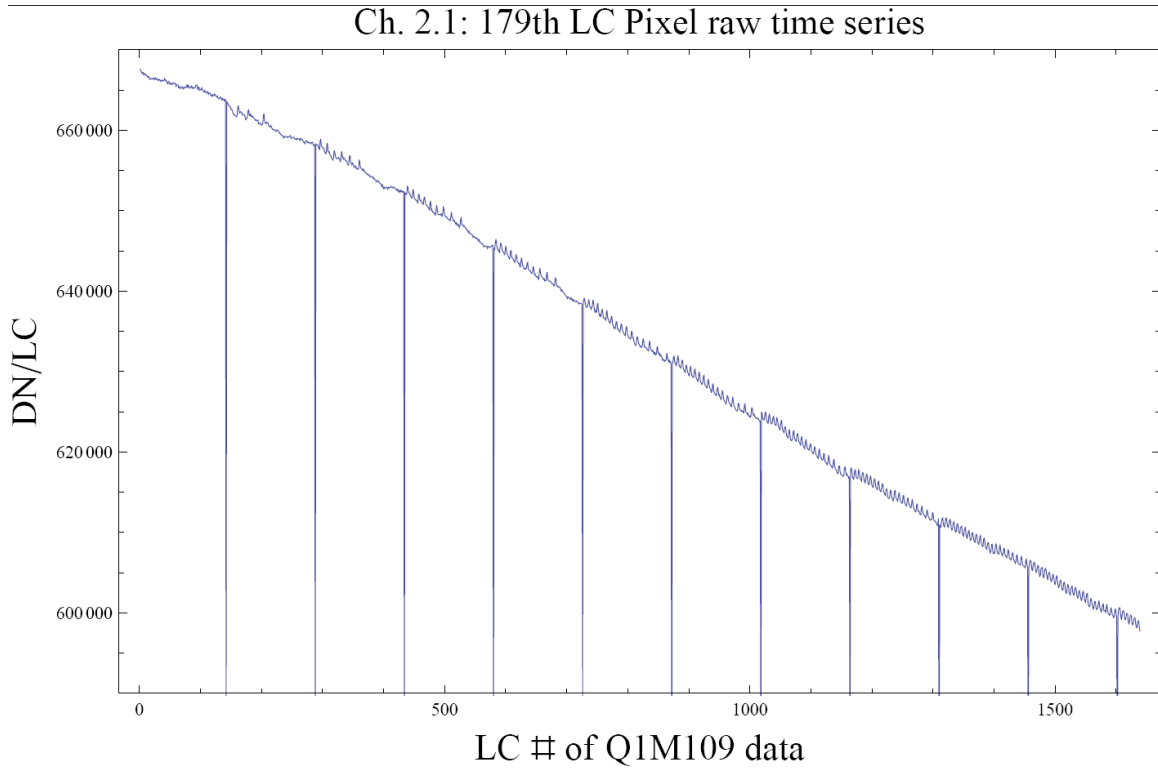


**Figure 8: A Good Example of the 3.2 hr Focus Oscillation in pixel time series data. Similar signatures are seen in flux and plate scale. The large negative-going spikes are caused by desaturations (Section 5.1), which have not removed from the time series. The abscissa is the Q1 relative cadence index, and the ordinate is Data Numbers (DN) per Long Cadence (LC).**

Reference: KAR-503 and KAR-527

### **5.8 Requantization Gaps**

Pixels at mean intensities  $>20,000$  e<sup>-</sup> show banding as shown in Figure 9, with quantized values of number of electrons preferred. This is most likely a result of the onboard requantization (KIH Section 7.4), and is considered benign since in the overall extraction the light curve is near the Poisson limit. However, it is noticeable in the data.

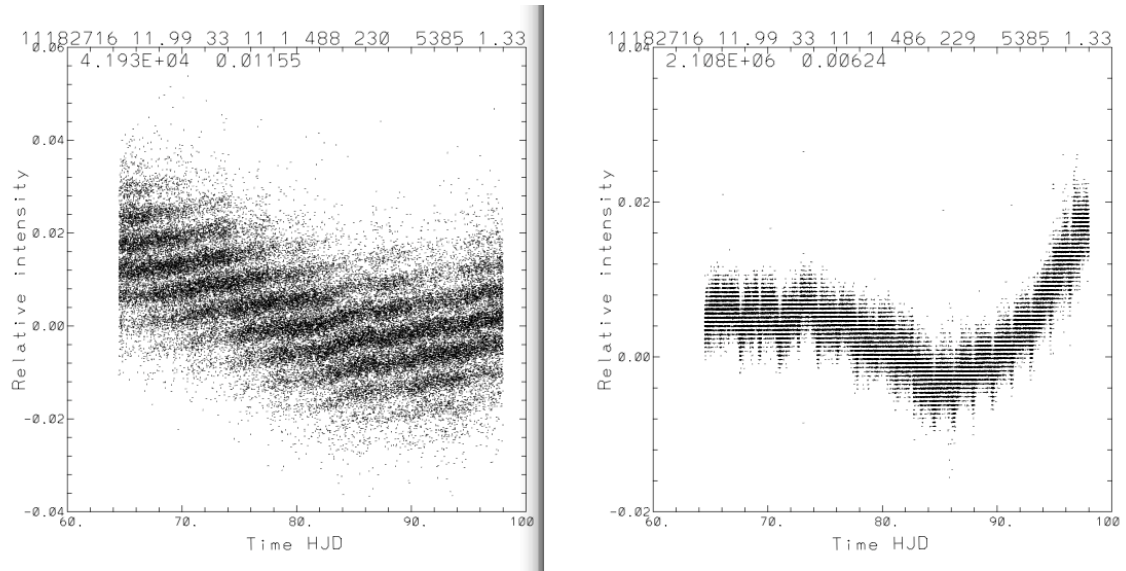


**Figure 9: Requantization gap example in Q1 SC pixel time series. The ‘band gaps’ scale with mean intensity (42,000 e- left, 2.1e6 right). See KIH Section 7.4 for a discussion of quantization and the (insignificant) information loss it entails.**

Reference: R. Gilliland, report dated 9/17/2009.

### **5.9 Spurious Frequencies in SC Data with Spacing of $1/LC$**

Spurious frequencies are seen in SC flux time series, and pixel data of all types – including black collateral pixels. The frequencies have an exact spacing of  $1/LC$  interval, as shown in Figure 10. As the SC data are analyzed in the frequency domain in order to measure the size and age of bright planetary host stars, the contamination of the data by these spurious frequencies will complicate these asteroseismology analyses, but will not compromise the core Kepler science. The physical cause of this problem is still under discussion, though the problem might be remedied with a simple comb notch filter in future releases even if no ancillary data can be found that exhibits these features.

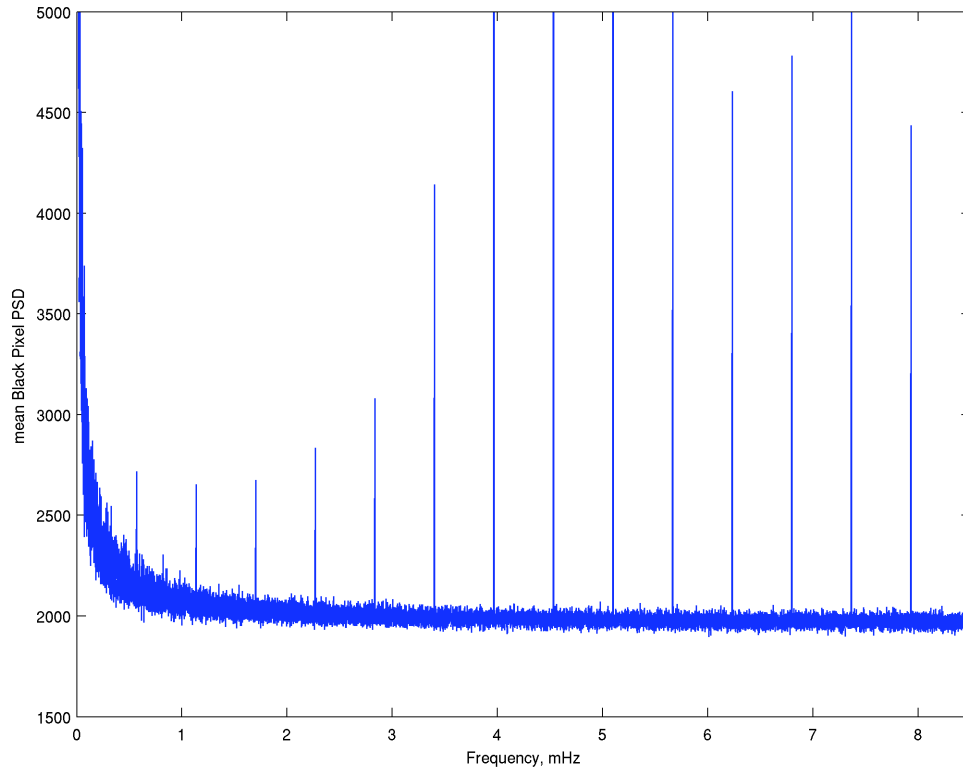


**Figure 10: Example of Spurious Frequencies seen in SC data. The fundamental at 0.56644 mHz (1/LC) can be easily seen here, as well as a comb of harmonics of this frequency.**

Reference: KAR-532

### ***5.10 Known Erroneous FITS header keywords***

The FFI WCS FITS header keywords are known to be incorrect. Users needing to locate sources seen in the FFIs are advised to use the pixel coordinate to sky coordinate tables in the KIH Supplement, which are reproduced in the Supplement to these Release Notes. These tables give the RA and DEC of each corner and the center of each channel, for each observing season; users may then interpolate to find the rough location of the source, and use star charts from other sources to precisely locate the object of interest.

It is not known if the WCS keywords in the pixel file headers are correct.

Reference: KAR-546.

## 6. Data Delivered – Format

Much of the material in this Section is from the MAST manual.

### 6.1 FFI

The FFIs are one FITS file per image, with 84 extensions, one for each module/output. See the KIH to map the extension table number = channel number onto module and output.

### 6.2 Light Curves

Light curves have file names like `kplr<kepler_id>-<stop_time>`, with a suffix of either `llc` (long cadence) or `slc` (short cadence), and a file name extension of `fits`.

A light curve is time series data, that is, a series of data points in time. Each data point corresponds to a measurement from a long cadence. For each data point, the flux value from simple aperture photometry (SAP) is given, along with the associated uncertainty. Only SAP light curves are available at this time. The centroid position for the target and time of the data point is also included.

The light curves are packaged as FITS binary table files. The fields of the binary table, all of which are scalar, are briefly described below and are listed in Table 8. The FITS header is listed in the Appendix of the MAST manual. Users wishing to identify the module and output on which a target is located must download the pixel data files or use MAST (for Q0 and Q1, select Module\_3 and Output\_3 as search outputs, for future Releases check the table shown at [http://archive.stsci.edu/kepler/kepler\\_fov/help/search\\_help.html](http://archive.stsci.edu/kepler/kepler_fov/help/search_help.html) to select the season number).

The following data values are given for each data point in a light curve:

- time of the data point
- for the simple aperture photometry (pixel sum) of optimal aperture pixels
  - first-moment centroid position of the target and uncertainty
  - raw flux value and uncertainty. Gap Cadences are set to -Inf
  - corrected un-filled flux value and uncertainty. Gap Cadences are set to -Inf

**Table 8: Available light curve data table fields, modified after the MAST manual: SAP replaces OAP, and data in columns 11-18 is not available and are filled with -Inf.**

Column Number	Field	Bytes	Description
1	time	4	Time from time series zero point (seconds)*
2	cad num	4	Cadence Interval Number (CIN)
Simple Aperture Photometry (SAP)			
3	row <sub>cent</sub>	4	row pixel location
4	$\sigma_{\text{row}}$	4	row position error
5	column <sub>cent</sub>	4	column pixel location
6	$\sigma_{\text{column}}$	4	column position error
7	raw flux	4	raw flux value
8	$\sigma_{\text{raw}}$	4	raw flux error
9	cal flux	4	corrected un-filled flux value

Column Number	Field	Bytes	Description
10	$\sigma_{\text{cal}}$	4	corrected un-filled flux error

\*Time in data table is Modified Julian Date in Release 2. The overwhelming consensus of the Science Team is to use solar system barycentric-corrected Julian Dates rather than MJD; this change will be implemented in the near future. See Section 6.4 for a discussion of time and time stamps.

In future Releases, the instrument magnitude flux value will provide an "Instrument magnitude flux time series" that is scaled to astronomically meaningful values as best they can be reconstructed. *Instrument Magnitude flux time series are not available at this time.*

If you are an IDL user, the `tbget` program in the `astrolib` library extracts the data. If you are an IRAF user, `tprint` can be used to dump an ascii table of selected row and column values.

### 6.3 Pixels

Target pixel data files are produced for *each target* from the calibrated data returned from the SOC. These are **not** cadence data, which contain all targets. Up to 5 different files are produced for each target. These consist of the long and short cadence pixel data for the target, the collateral pixels for the long and short cadences, and the background pixels

Both original pixel values and calibrated flux values are in the pixel data files. The original pixel value is the integer value as recorded on the spacecraft. The calibrated pixel value is that provided by the SOC. Oddly enough, the sum of calibrated pixel values is called the 'raw' light curve value.

The original and flux calibrated values are listed for each pixel.

The target pixel data files are archived as a dataset. A request for the data will return all extensions that were archived with the dataset.

Pixel data table fields are described in the Kepler Archive Manual (KDMC-10008).

## 6.4 Time and Time Stamps

### 6.4.1 Overview

The precision and accuracy of the time assigned to an event observed by Kepler are limited by the intrinsic precision and accuracy of the hardware, the promptness and reproducibility of the flight software time-stamping process, and by the SNR of the target. The Flight System requirement, including both hardware and software contributions, is that the absolute time of the start and end of each cadence is known to  $\pm 50$  ms. This requirement was developed so that knowledge of event times would be limited by the characteristics of the event, rather than the characteristics of the flight system.

Several factors must be accounted for before approaching the 50 ms limit:

1. Relate readout time of a pixel to Vehicle Time Code (VTC) recorded for that pixel and cadence in the SSR. The VTC stamp of a cadence is created within 4 ms after the last pixel of the last frame of the last time slice of that cadence is read out from the LDE.
2. VTC to UTC of end of Cadence, using Time Correlation Coefficients. Done by DMC, with precision and accuracy to be documented.

3. Convert UTC to Barycentric JD. While PA generates per-target barycentric correction time series, these are not used in the light curve FITS files in Release 2. Users wishing to perform their own barycentric corrections should see Section 6.4.3.
4. Add time slice offsets (See KIH Section 5.1). Not done in Release 2. The amplitude of the time slice offset can be up to 3 s. Users wishing to perform their own time slice corrections should see Section 6.4.4.

**6.4.2 What’s in the Light Curve FITS Header in Release 2**

The Release 2 light curve headers contain

1. A start and end timestamp in MJD stored in FITS Keywords LC\_START and LC\_END. Both Long and Short Cadence light curves use this same keyword, since in this instance ‘LC’ is mnemonic for ‘Light Curve’ rather than indicating Long Cadence.
2. A field with a valid entry for every ungapped cadence in the data table. It is single precision seconds from LC\_START, and refers to the MJD midpoint of the Cadence.

No barycentric or time slice correction is applied to the start/end times or the Cadence times.

**6.4.3 Do your own Barycentric Correction**

The amplitude of the barycentric correction is approximately  $(a_E/c)\cos\beta$ , where  $a_E$  is the semi-major axis of Earth,  $c$  the speed of light, and  $\beta$  is the ecliptic latitude of the target. In the case of the center of the Kepler FOV, with  $\beta = 65$  degrees, the amplitude of the UTC to barycentric correction is approximately +/- 211 s. BJD is later than UTC when Kepler is on the half of its orbit closest to Cygnus (roughly May 1 – Nov 1) and earlier than UTC on the other half of the orbit. Because of the large Kepler FOV, the barycentric correction must be performed on a channel-by-channel basis, and on a target-by-target basis if accuracy within 10 s is required. Users content with errors up to 8s/degree away from the FOV center may use Table 9, which presents the barycentric correction for a target at FOV center (ecliptic longitude = 307°, latitude = 65°) using the Kepler spacecraft ephemeris from HORIZONS (<http://ssd.jpl.nasa.gov/?horizons>). Directions for calculating more accurate corrections are given below the Table.

**Table 9: Kepler FOV center Barycentric correction**

<b>Kepler FOV center Barycentric correction</b>			Target co-ordinates			
			ecl. lat	65	d	
			ecl. long	307	d	
		Add dt to JD to get BJD	Unit vector to target			
			X	Y	Z	
				0.254	-0.338	0.906
			Kepler Cartesian coordinates in AU			
JD	Calendar (Oh)	MJD	X	Y	Z	dt (s)
2454952.5	2009-May-01	54952	-0.802	-0.647	0.007	10.4
2454953.5	2009-May-02	54953	-0.791	-0.660	0.007	13.9
2454954.5	2009-May-03	54954	-0.781	-0.673	0.007	17.5
2454955.5	2009-May-04	54955	-0.770	-0.686	0.007	21.0
2454956.5	2009-May-05	54956	-0.759	-0.698	0.007	24.6
2454957.5	2009-May-06	54957	-0.748	-0.711	0.007	28.1
2454958.5	2009-May-07	54958	-0.737	-0.723	0.007	31.6
2454959.5	2009-May-08	54959	-0.725	-0.735	0.008	35.1

**Kepler FOV center Barycentric correction**

Target co-ordinates

ecl. lat           65 d

ecl. long         307 d

Add dt to JD to get BJD

Unit vector to target

X                Y           Z

0.254   -0.338   0.906

Kepler Cartesian coordinates in AU

JD	Calendar (Oh)	MJD	X	Y	Z	dt (s)
2454960.5	2009-May-09	54960	-0.714	-0.747	0.008	38.6
2454961.5	2009-May-10	54961	-0.702	-0.759	0.008	42.1
2454962.5	2009-May-11	54962	-0.690	-0.770	0.008	45.6
2454963.5	2009-May-12	54963	-0.677	-0.781	0.008	49.1
2454964.5	2009-May-13	54964	-0.665	-0.792	0.008	52.6
2454965.5	2009-May-14	54965	-0.652	-0.803	0.008	56.0
2454966.5	2009-May-15	54966	-0.639	-0.814	0.008	59.4
2454967.5	2009-May-16	54967	-0.626	-0.824	0.008	62.8
2454968.5	2009-May-17	54968	-0.613	-0.834	0.008	66.2
2454969.5	2009-May-18	54969	-0.600	-0.844	0.008	69.6
2454970.5	2009-May-19	54970	-0.586	-0.854	0.008	73.0
2454971.5	2009-May-20	54971	-0.573	-0.864	0.008	76.3
2454972.5	2009-May-21	54972	-0.559	-0.873	0.008	79.6
2454973.5	2009-May-22	54973	-0.545	-0.882	0.008	82.9
2454974.5	2009-May-23	54974	-0.531	-0.891	0.008	86.2
2454975.5	2009-May-24	54975	-0.517	-0.899	0.008	89.5
2454976.5	2009-May-25	54976	-0.502	-0.908	0.008	92.7
2454977.5	2009-May-26	54977	-0.488	-0.916	0.008	95.9
2454978.5	2009-May-27	54978	-0.473	-0.924	0.008	99.1
2454979.5	2009-May-28	54979	-0.459	-0.931	0.008	102.2
2454980.5	2009-May-29	54980	-0.444	-0.939	0.008	105.3
2454981.5	2009-May-30	54981	-0.429	-0.946	0.008	108.4
2454982.5	2009-May-31	54982	-0.414	-0.953	0.008	111.5
2454983.5	2009-Jun-01	54983	-0.399	-0.959	0.008	114.5
2454984.5	2009-Jun-02	54984	-0.383	-0.966	0.008	117.6
2454985.5	2009-Jun-03	54985	-0.368	-0.972	0.008	120.5
2454986.5	2009-Jun-04	54986	-0.352	-0.978	0.008	123.5
2454987.5	2009-Jun-05	54987	-0.337	-0.983	0.008	126.4
2454988.5	2009-Jun-06	54988	-0.321	-0.989	0.008	129.3
2454989.5	2009-Jun-07	54989	-0.305	-0.994	0.008	132.1
2454990.5	2009-Jun-08	54990	-0.290	-0.998	0.008	134.9
2454991.5	2009-Jun-09	54991	-0.274	-1.003	0.008	137.7
2454992.5	2009-Jun-10	54992	-0.258	-1.007	0.008	140.4
2454993.5	2009-Jun-11	54993	-0.242	-1.011	0.008	143.2
2454994.5	2009-Jun-12	54994	-0.226	-1.015	0.008	145.8
2454995.5	2009-Jun-13	54995	-0.209	-1.019	0.008	148.4

**Kepler FOV center Barycentric correction**

			Target co-ordinates			
			ecl. lat	65	d	
			ecl. long	307	d	
	Add dt to JD to get BJD		Unit vector to target			
			X	Y	Z	
			0.254	-0.338	0.906	
			Kepler Cartesian coordinates in AU			
JD	Calendar (Oh)	MJD	X	Y	Z	dt (s)
2454996.5	2009-Jun-14	54996	-0.193	-1.022	0.008	151.0
2454997.5	2009-Jun-15	54997	-0.177	-1.025	0.008	153.6
2454998.5	2009-Jun-16	54998	-0.161	-1.028	0.008	156.1
2454999.5	2009-Jun-17	54999	-0.144	-1.030	0.008	158.6

Users can do their own correction for specific targets using the Kepler ephemeris included in the Supplement. The barycentric correction is

$$\Delta t_B = BJD - JD = \hat{L} \cdot \vec{r}_{AU}$$

$$\hat{L} = (\cos \beta \cos \lambda, \cos \beta \sin \lambda, \sin \beta)$$

where  $\hat{L}$  is the unit vector pointing towards the target at ecliptic longitude  $\lambda$  and latitude  $\beta$ ,  $\vec{r}$  is the Cartesian coordinates of Kepler (in a system in which X = first point of Aries, Z = ecliptic pole, and units are AU – the default supplied by Horizons), and  $t_{AU}$  = light travel time for 1 AU = 499.0 s.

Users wishing to download their own Kepler ephemeris can do this:

1. Telnet into Horizons port on the ssd server: `telnet ssd.jpl.nasa.gov 6775`
2. Enter the spacecraft code -227 at the prompt.
3. Select ephemeris → vectors
4. Enter barycenter ID (@0) at the Coordinate center prompt
5. Reference plane: `eclip(tic)`
6. Enter start and stop times and desired output interval
7. Accept default output
8. Email the results to yourself.

**6.4.4 Do your own Time Slice Correction**

Users wishing to do their own time slice correction should look up the module and output of their target in MAST, identify the time slice from the Detector Properties Table (Table 13) of the Instrument Handbook, and subtract  $0.25 + 0.62(5 - n_{\text{slice}})$  s from the BJD, where  $n_{\text{slice}}$  is the time slice index (1-5). Note that this correction is NOT the same from Quarter to Quarter, so it is necessary to apply the time slice correction even when considering intervals between Cadences.

#### **6.4.5 Caveats and Uncertainties**

Factors, in addition to the possibility of mistakes, which users should consider before basing scientific conclusions on time stamps and do-it-yourself corrections are:

1. The precise phasing of an individual pixel with respect to the cadence time stamp (not understood to better than  $\pm 0.5$  s)
2. Relativistic effects in the calculation of the barycentric correction.

The advice of the DAWG is not to consider as scientifically significant relative timing variations less than one frame time (6.5 s) or absolute timing accuracy better than one SC period (58.8 s) until such time as the stability and accuracy of time stamps can be documented to near the theoretical limit. The DAWG expects this documentation to be available for Release 3.

## 7. References

1. "Initial Assessment Of The Kepler Photometric Precision," W.J. Borucki, NASA Ames Research Center, J. Jenkins, SETI Institute, and the Kepler Science Team (May 30, 2009)
2. "Kepler's Optical Phase Curve of the Exoplanet HAT-P-7," W. J. Borucki, Science Vol 325 7 August 2009 p. 709

## 8. List of Acronyms and Abbreviations

ACS	Advanced Camera for Surveys
ADC	Analog to Digital Converter
ADCS	Attitude Determination and Control Subsystem
ARP	Artifact Removal Pixel
BATC	Ball Aerospace & Technologies Corp.
BG	BackGround pixel of interest
BOL	Beginning Of Life
BPF	Band Pass Filter
CAL	Pixel Calibration CSCI
CCD	Charge Coupled Device
CDPP	Combined Differential Photometric Performance
CDS	Correlated Double Sampling
CR	Cosmic Ray
CSCI	Computer Software Configuration Item
CTE	Charge Transfer Efficiency
CTI	Charge Transfer Inefficiency
DAA	Detector Array Assembly
DAP	Data Analysis Program
DCA	Detector Chip Assembly
DCE	Dust Cover Ejection
DIA	Differential Image Analysis
DMC	Data Management Center
DNL	Differential Non-Linearity of A/D converter
DSN	Deep Space Network
DV	Data Validation CSCI
DVA	Differential Velocity Aberration
ECA	Electronic Component Assembly
EE	Encircled Energy
EOL	End of Life
ETEM	End-To-End Model of Kepler
FFI	Full Field Image
FFL	Field Flattener Lens
FGS	Fine guidance sensor
FOP	Follow-up Observation Program
FOV	Field of View
FPA	Focal Plane Assembly
FPAA	Focal Plane Array Assembly
FSW	Flight Software

GCR	Galactic Cosmic Ray
GO	Guest Observer
GUI	Graphical User Interface
HGA	high-gain antenna
HST	Hubble Space Telescope
HZ	Habitable Zone
I&T	Integration and Test
INL	Integral Non-Linearity of A/D converter
IRNU	Intra-pixel Response Nonuniformity
KACR	Kepler Activity Change Request (for additional data during Commissioning)
KCB	Kepler Control Box
KDAH	Kepler Data Analysis Handbook
KIC	Kepler Input Catalog
KTD	Kepler Tech Demo simulated star field light source
LC	Long Cadence
LCC	Long Cadence Collateral
LDE	Local Detector Electronics
LGA	low-gain antenna
LOS	Line of Sight
LPS	LDE Power Supply
LUT	look-up table
LV	Launch Vehicle
MAD	Median Absolute Deviation
MAST	Multi-mission Archive at STSci
MJD	Modified Julian Date = JD - 2400000.5
MOC	Mission Operation Center
MORC	Module, Output, Row, Column
NVM	Non-Volatile Memory
OFAD	Optical Field Angle Distortion
PA	Photometric Analysis CSCI
PDC	Pre-Search Data Conditioning CSCI
PID	Pipeline instance Identifier (unique number assigned to each run of the Pipeline)
PM	Primary Mirror
PMA	Primary Mirror Assembly
POI	Pixels of Interest
ppm	parts per million
PRF	Pixel Response Function
PRNU	Pixel Response Non-Uniformity

PSD	power spectral density
PSF	Point Spread Function
PSP	Participating Scientist Program
PWA	Printed Wiring Assembly
QE	Quantum Efficiency
RC	Reverse Clock
S/C	Spacecraft
S/W	Software
SAO	Smithsonian Astrophysical Observatory
SC	Short Cadence
SCo	Schmidt Corrector
SDA	Science Data Accumulator
SNR	signal-to-noise
SO	Science Office
SOC	Science Operations Center
SOL	Start-of-Line
SSR	Solid State Recorder
SSTVT	Single-String Transit Verification Test
STScI	Space Telescope Science Institute
SVD	Singular Value Decomposition
TAD	Target and Aperture Definition CSCI
TDT	Target Definition Table
TPS	Terrestrial Planet Search CSCI
TVAC	Thermal Vacuum testing

## 9. Contents of Supplement

The Supplement is available as a full package (DataReleaseNotes\_02\_SupplementFull.tar) and a short package suitable for emailing (DataReleaseNotes\_02\_SupplementSmall.tar). Here is the README file listing the contents of the full Supplement:

### Data Release 2 Notes Supplement Files

File Name	Contents
ArgAgg_Q0_LC_PID278_MADT010_MCT10_ArgStatsAll.txt	Argabrightening statistic for all channels and cadences, corresponding to Table 4
ArgAgg_Q0_LC_PID278_MADT010_MCT10_Summary.txt	Argabrightening multichannel event summary, same as Table 4
ArgAgg_Q0_SC_PID338_MADT010_MCT10_ArgStatsAll.txt	Argabrightening statistic for all channels and cadences, corresponding to Table 5
ArgAgg_Q0_SC_PID338_MADT010_MCT10_Summary.txt	Argabrightening multichannel event summary, same as Table 5
ArgAgg_Q1_LC_PID359_MADT010_MCT10_ArgStatsAll.txt	Argabrightening statistic for all channels and cadences, corresponding to Table 6
ArgAgg_Q1_LC_PID359_MADT010_MCT10_Summary.txt	Argabrightening multichannel event summary, same as Table 6
ArgAgg_Q1_SC_PID379_MADT010_MCT10_ArgStatsAll.txt	Argabrightening statistic for all channels and cadences, corresponding to Table 7
ArgAgg_Q1_SC_PID379_MADT010_MCT10_Summary.txt	Argabrightening multichannel event summary, same as Table 7
Kepler_Barycentric_Ephemeris.txt	Cartesian barycentric coordinates of Kepler spacecraft
prf_ch_01-prf_ch_84.fits	Centered-pixel Pixel Response Function for each of the 84 channels
Q0Q1_EB_Var1_Var2_MJD_gap.txt	FGS variable star flux telemetry
Q0Q1_TH1RW34T_MJD_gap.txt	Reaction wheel thermistor telemetry
Q0_LC_isNotFinePoint.txt	Long Cadences which were not in Fine Point, same as Table 2 (upper)
Q0_SC_isNotFinePoint.txt	Short Cadences which were not in Fine Point
Q1_LC_isNotFinePoint.txt	Long Cadences which were not in Fine Point, same as Table 2 (lower)
Q1_PPA_STELLAR.txt	List of PPA_STELLAR KeplerIds (PRF centroiding)
Q1_SC_isNotFinePoint.txt	Short Cadences which were not in Fine Point
morc_2_ra_dec_4_seasons.txt	(Module, Output, Row, Column) to (RA, DEC) conversion for each of the 4 seasons

Here are the files in the short package:

```
ArgAgg_Q0_LC_PID278_MADT010_MCT10_ArgStatsAll.txt
ArgAgg_Q0_LC_PID278_MADT010_MCT10_Summary.txt
ArgAgg_Q0_SC_PID338_MADT010_MCT10_Summary.txt
ArgAgg_Q1_LC_PID359_MADT010_MCT10_ArgStatsAll.txt
ArgAgg_Q1_LC_PID359_MADT010_MCT10_Summary.txt
ArgAgg_Q1_SC_PID379_MADT010_MCT10_Summary.txt
Kepler_Barycentric_Ephemeris.txt
Q0_LC_isNotFinePoint.txt
Q0_SC_isNotFinePoint.txt
Q1_LC_isNotFinePoint.txt
Q1_PPA_STELLAR.txt
Q1_SC_isNotFinePoint.txt
README.txt
morc_2_ra_dec_4_seasons.txt
prf_ch_01-prf_ch_84.fits
```